Supporting Information

Direct analysis at temporal and molecular-level of deactivating coke species formed on zeolite catalysts with diverse pore topologies

Idoia Hita,[a] Hend Omar Mohamed,[a] Yerrayya Attada,[a] Naydu Zambrano,[a] Wen Zhang,[b] Adrian Ramírez,[c] Pedro Castaño,[a]*

[a] *Multiscale Reaction Engineering, KAUST Catalysis Center (KCC), King Abdullah University of Science and Technology, Thuwal 23955-6900, Saudi Arabia.*

[b] *King Abdullah University of Science and Technology, Imaging and Characterization Core Labs, Thuwal 23955, Saudi Arabia*

[c] *King Abdullah University of Science and Technology, KAUST Catalysis Center (KCC), Thuwal 23955, Saudi Arabia*

* Corresponding author*:* *pedro.castano@kaust.edu.sa*

Supplementary Figures

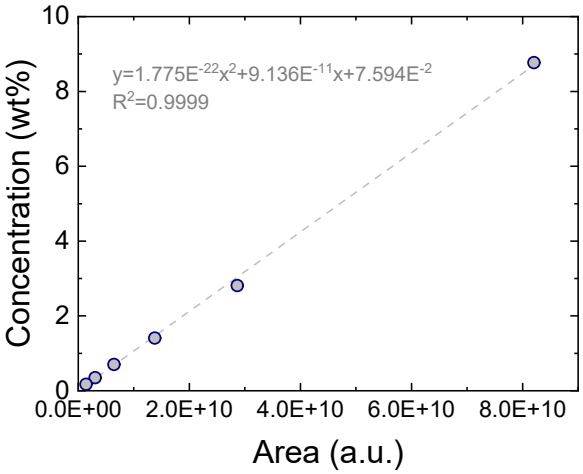

Figure S1 Calibration curve used to calculate the soluble coke concentration.

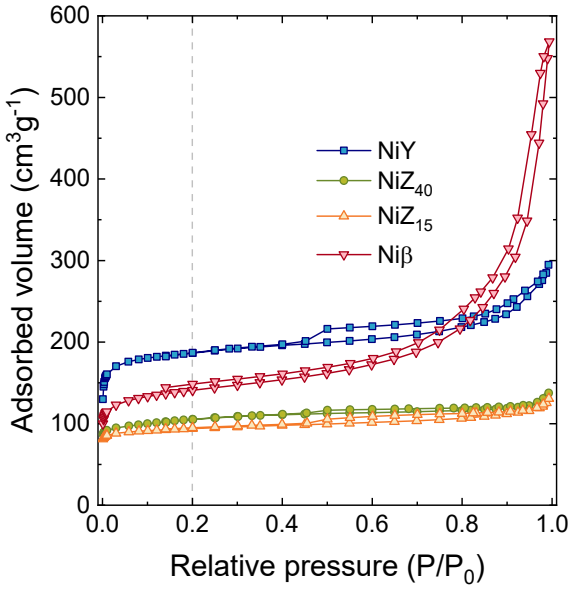

Figure S2. N_2 adsorption-desorption isotherm for all fresh zeolite-based catalysts.

The bimodal distributions of the NH_3-TPD profiles (Figure S3) allow their Gaussian deconvolutions to estimate the contributions of the different types of acidity in the catalysts, namely a mild acidity (a_1) and a stronger acidity (a_2) presenting a higher temperature NH_3 desorption peak. The temperatures of the maximum values of each peak are designated as T_1 and T_2, respectively. Overall, the NiZ_{15} catalyst (the most acidic) has the highest proportion of weaker acidic sites (70.6 %). While the weaker acidity peaks for the NiY, NiZ_{15}, and NiZ_{40} catalysts have maxima at T_1 = 281-292 °C, the same peak for the Niß catalyst presents its maximum at T_1 = 257 °C, indicating a weaker nature for the a_1 sites by comparison. This is analogous to what is observed for the a_2 acidic sites, where the maximum for the Niß peak is located at 341 °C, 23-42 °C less than for the higher acidity peaks of the other catalysts. This denotes that the Niß catalyst has the overall weakest acidic sites of all the studied catalysts.

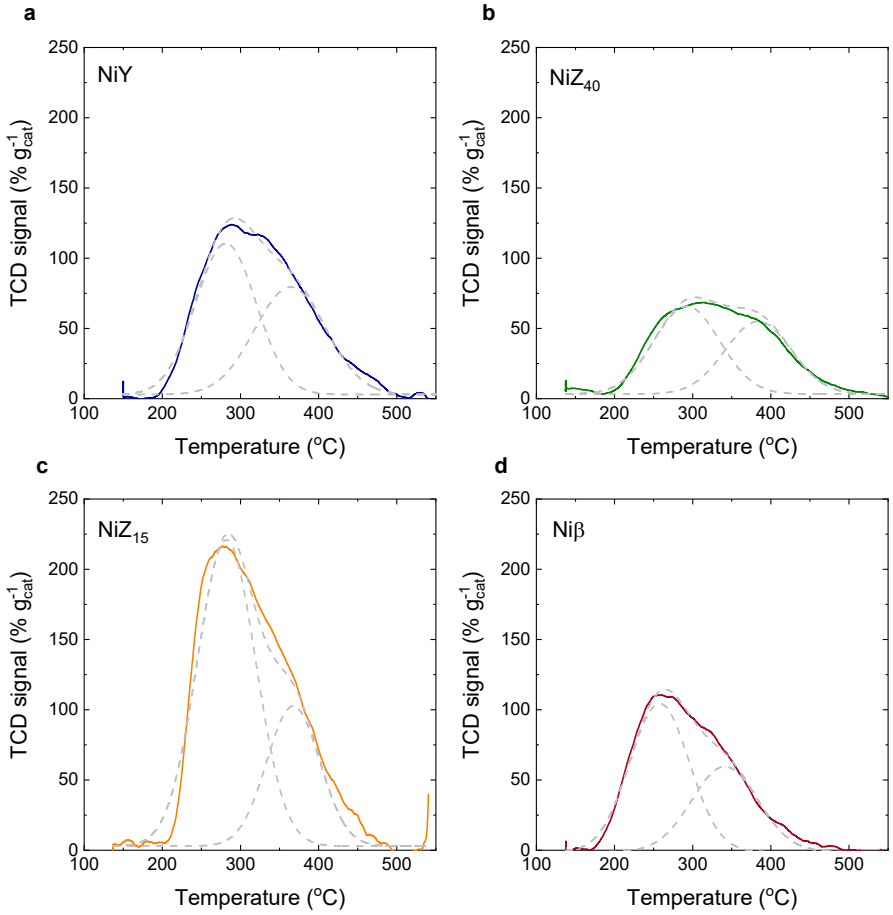

Figure S3 Deconvolution of the NH_3-TPD curves for all zeolite-based catalysts.

The acid properties were further investigated by pyridine adsorption infrared spectra (Figure S4). All catalysts exhibit three different peaks at the ~1545, ~1455, and 1491 cm^{-1} bands that are attributed to the Brønsted acid sites (BASs), Lewis acid sites (LASs), and contributions from both the Brønsted and Lewis acid sites, respectively. The measured BAS and LAS contributions agree with the acidity properties determined by NH_3-TPD (see Table S1), where the Niß catalyst shows the highest amount of LAS (1088 µmol g^{-1}), followed by NiZ_{40} (546 µmol g^{-1}), NiZ_{15} (380 µmol g^{-1}), and finally NiY (82 µmol g^{-1}). This high LAS amount of the Niß catalyst is attributed to a significant presence of non-framework Si-OH or Al-OH on the surface [1]. Conversely, the NiY catalyst exhibits the highest BAS amount (131 µmol g^{-1}). All in all, the NiY catalyst presents the highest BAS/LAS ratio followed by the NiZ_{15}, NiZ_{40}, and Niß catalysts.

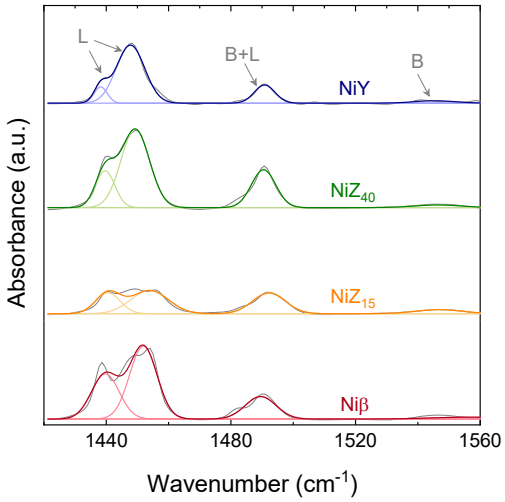

Figure S4 Infrared spectra of pyridine adsorption on the fresh catalysts.

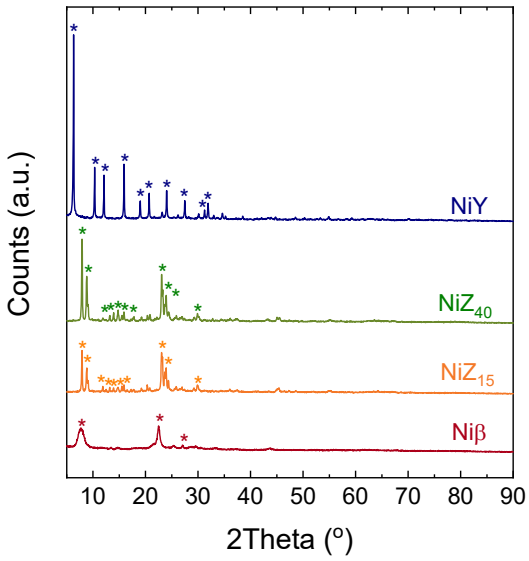

Figure S5 XRD patterns for all fresh catalysts.

The NiY catalyst (Figure S6a) shows a regular octahedral crystal morphology with a particle size of 400 ± 130 nm. The NiZ_{15} and NiZ_{40} catalysts (Figs. S6b-c) present similar morphologies of irregular hexagonal crystals with average particle sizes of 210 ± 87 nm and 320 ± 85 nm, respectively. Lastly, the Niß catalyst (Figure S6d) shows spherical nano-crystallites with sizes between 80 and 100 nm that are clustered in agglomerates of about 200–500 nm.

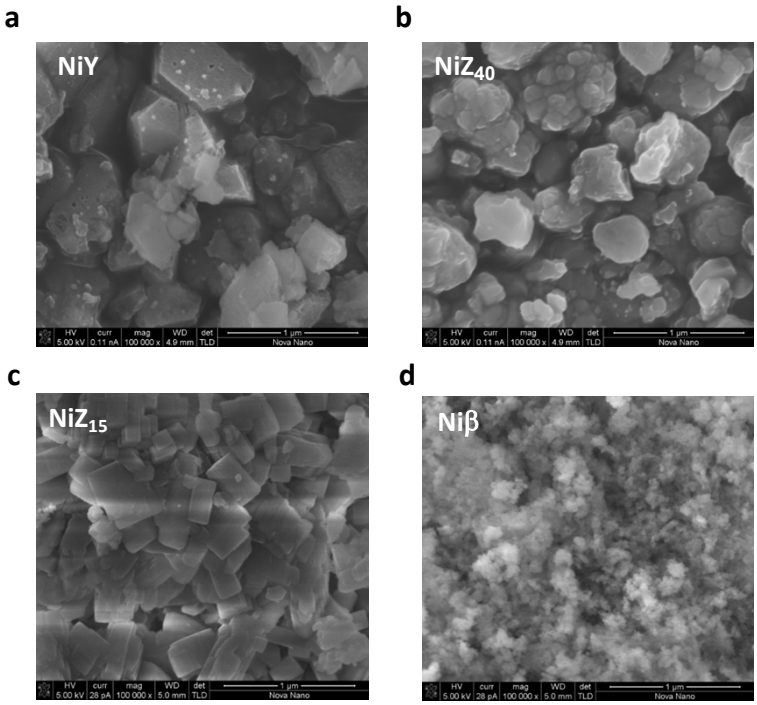

Figure S6 SEM images for the fresh catalysts.

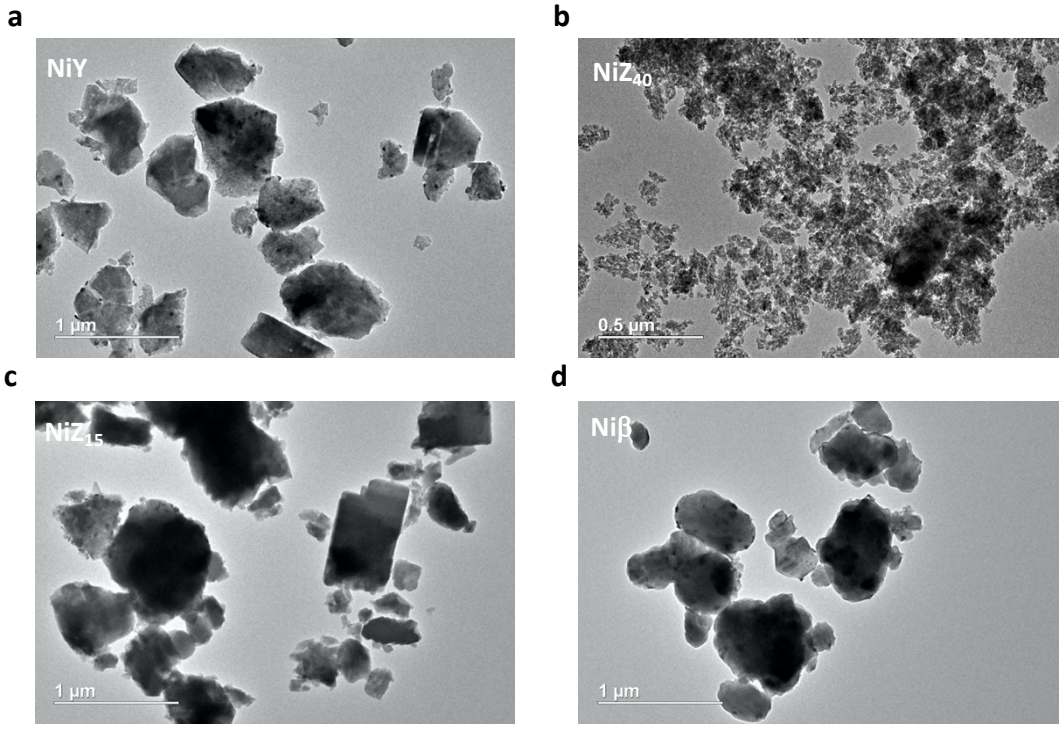

Figure S7 TEM images for the fresh catalysts.

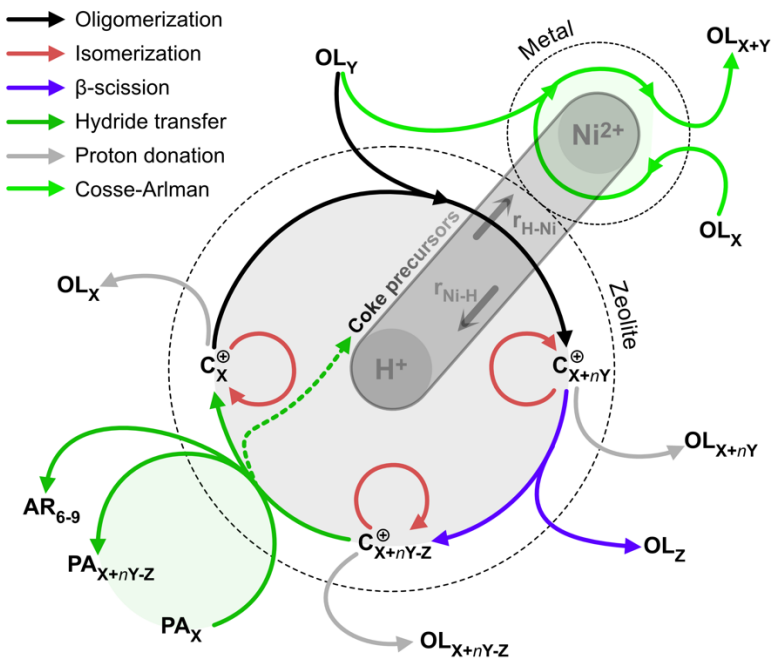

Figure S8 Schematization of the proposed ethylene oligomerization mechanism over the Ni/zeolite catalysts.

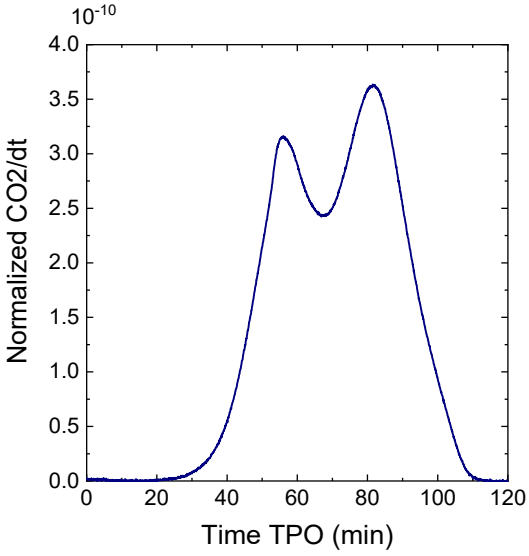

Figure S9 Representative CO_2 profile from the TG-TPO/MS analysis of the deactivated NiY catalyst after 10 h on stream.

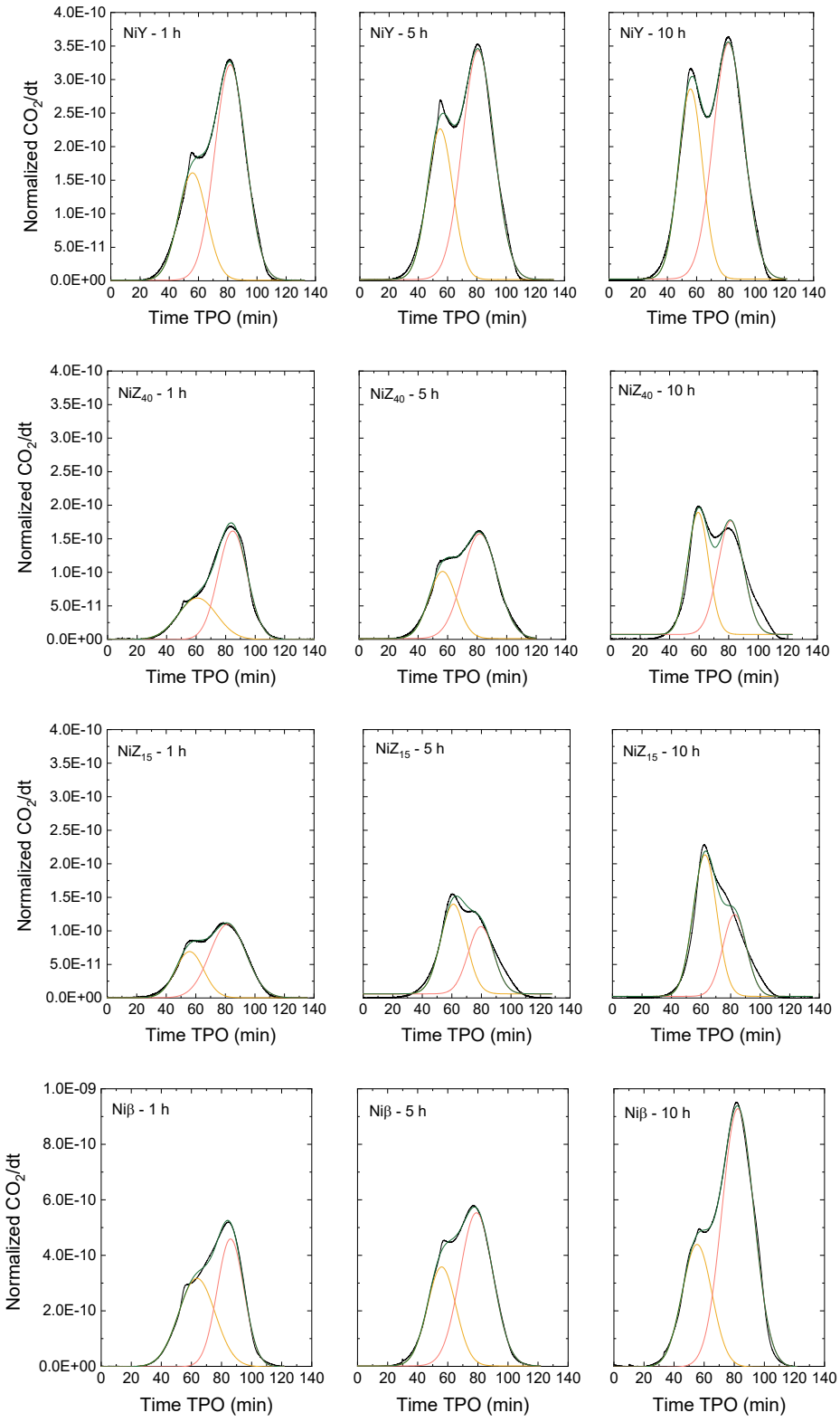

Figure S10 Gaussian deconvolutions of the CO_2 profiles from the TG-TPO/MS analysis of the deactivated catalyst samples at different times on stream.

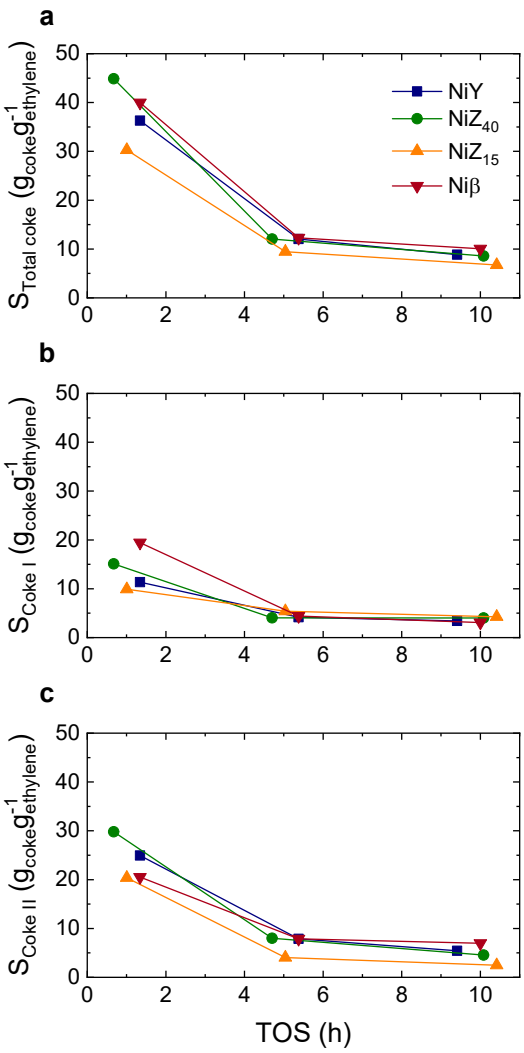

Figure S11 Selectivity evolution towards a) total coke, b) coke I, and c) coke II over time on stream for all catalysts.

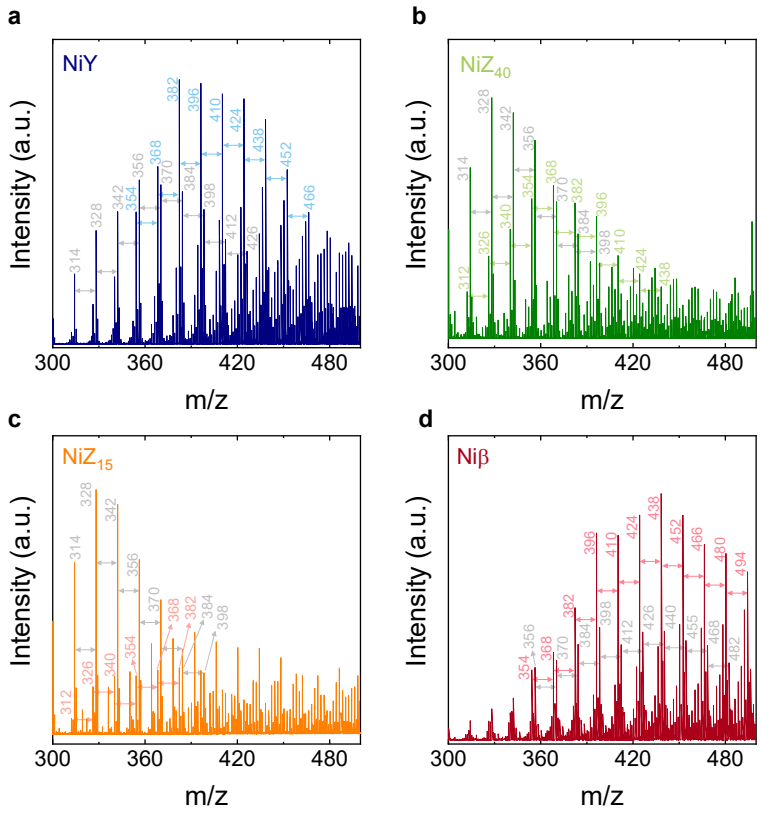

Figure S12 LDI FT-ICR/MS signals in the m/z = 300-500 range for all catalysts deactivated at a time on stream of 5h.

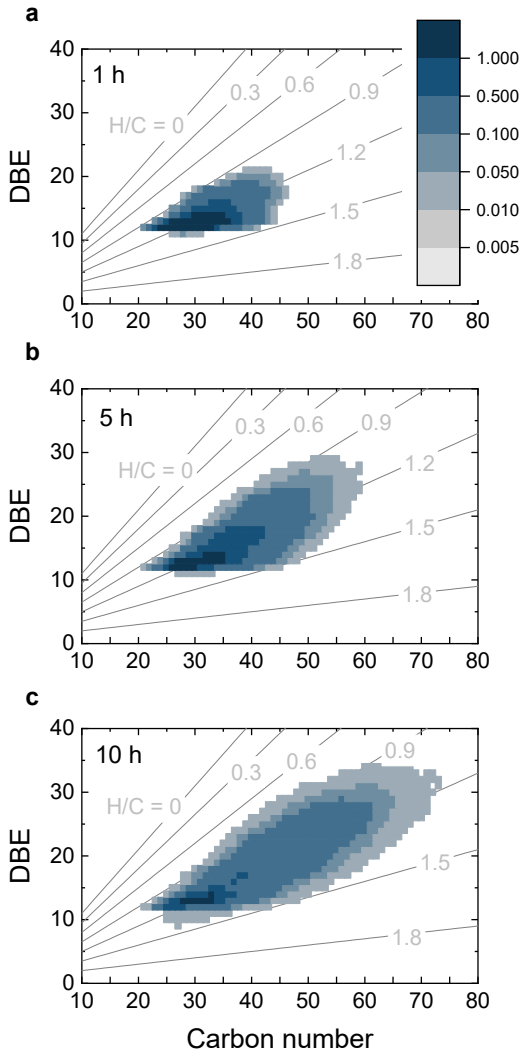

Figure S13 Color-coded isoabundance plots for the total cokes formed at a) 1 h, b) 5 h, and c) 10 h on stream using the NiY catalyst. Darker colors represent higher species concentration while lighter colors represent lower concentrations (in a logarithmic scale).

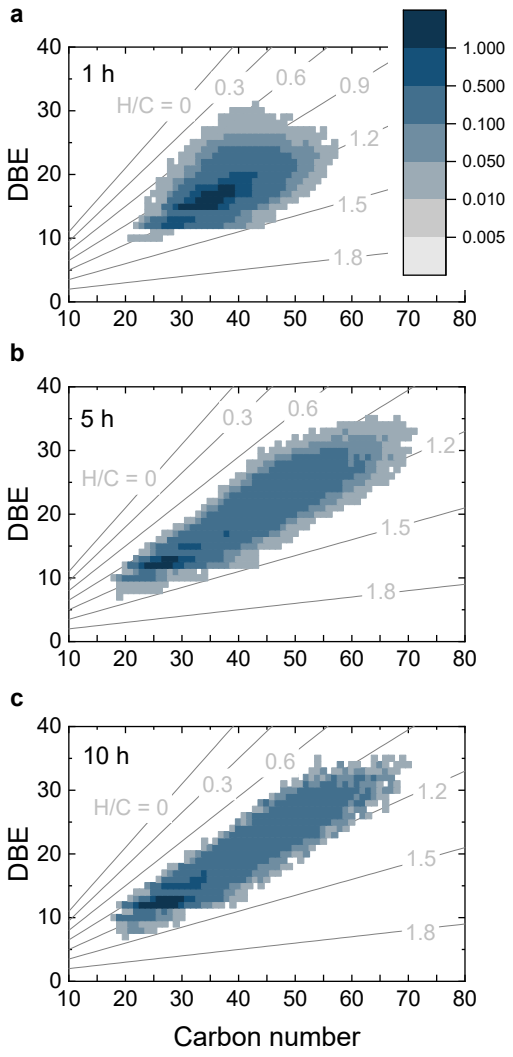

Figure S14 Color-coded isoabundance plots for the total cokes formed at a) 1 h, b) 5 h, and c) 10 h on stream using the NiZ_{40} catalyst. Darker colors represent higher species concentration, while lighter colors represent lower concentrations (in a logarithmic scale).

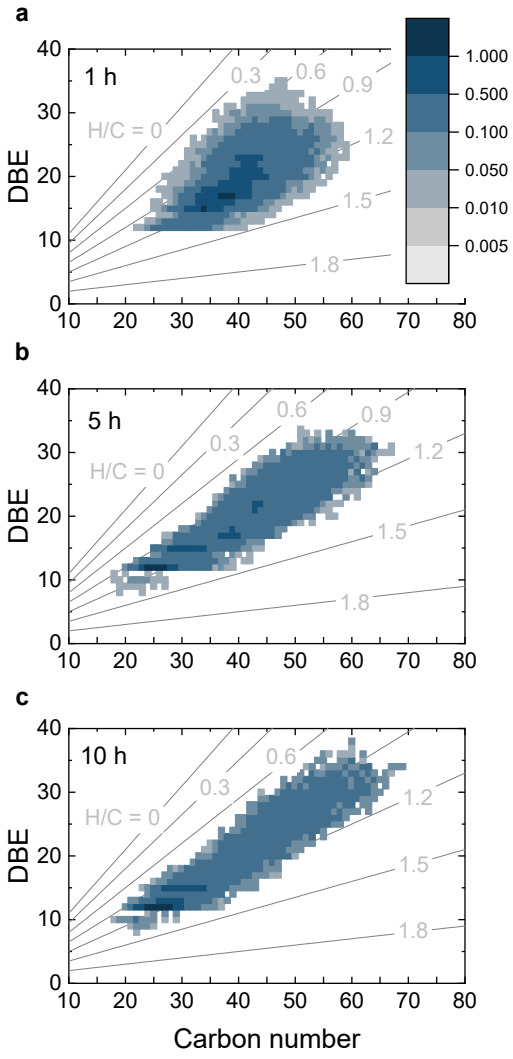

Figure S15 Color-coded isoabundance plots for the total cokes formed at a) 1 h, b) 5 h, and c) 10 h on stream using the NiZ_{15} catalyst. Darker colors represent higher species concentration while lighter colors represent lower concentrations (in a logarithmic scale).

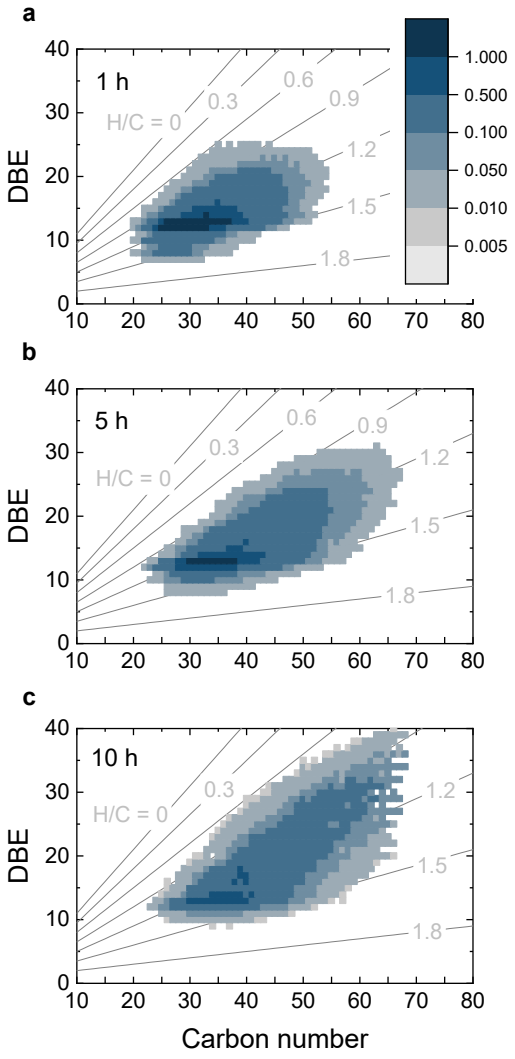

Figure S16 Color-coded isoabundance plots for the total cokes formed at a) 1 h, b) 5 h, and c) 10 h on stream using the Niβ catalyst. Darker colors represent higher species concentration while lighter colors represent lower concentrations (in a logarithmic scale).

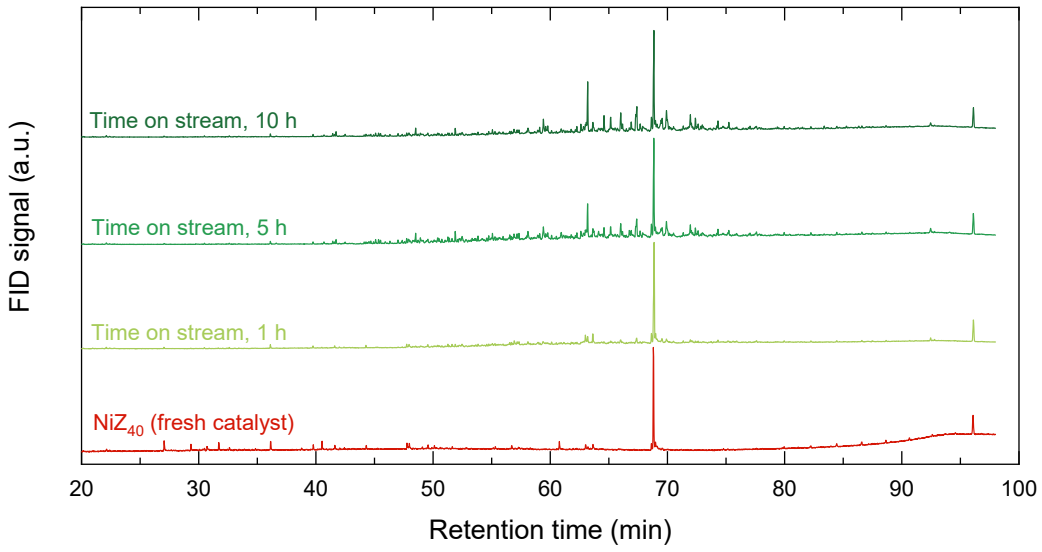

Figure S17 Chromatograms obtained from the GC analysis of the soluble cokes formed in the NiZ_{40} catalyst at different times on stream. The signal at the bottom corresponds to the extract obtained from applying the coke extraction protocol on a fresh (non-reacted) NiZ_{40} catalyst, which was used to discern the GC peaks corresponding to coke species from those which have a zeolitic origin.

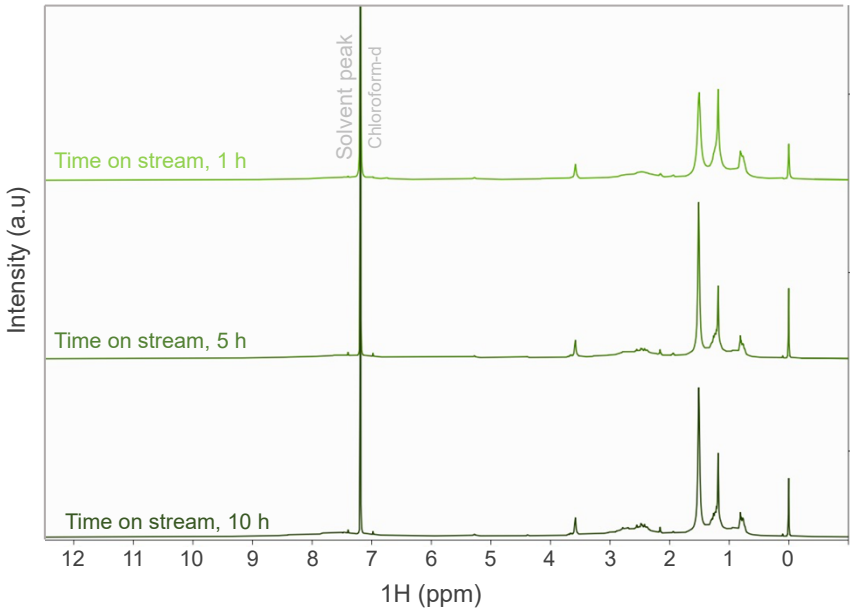

Figure S18 ^{1}H NMR spectrum of soluble cokes formed in the NiZ_{40} catalyst at different times on stream.

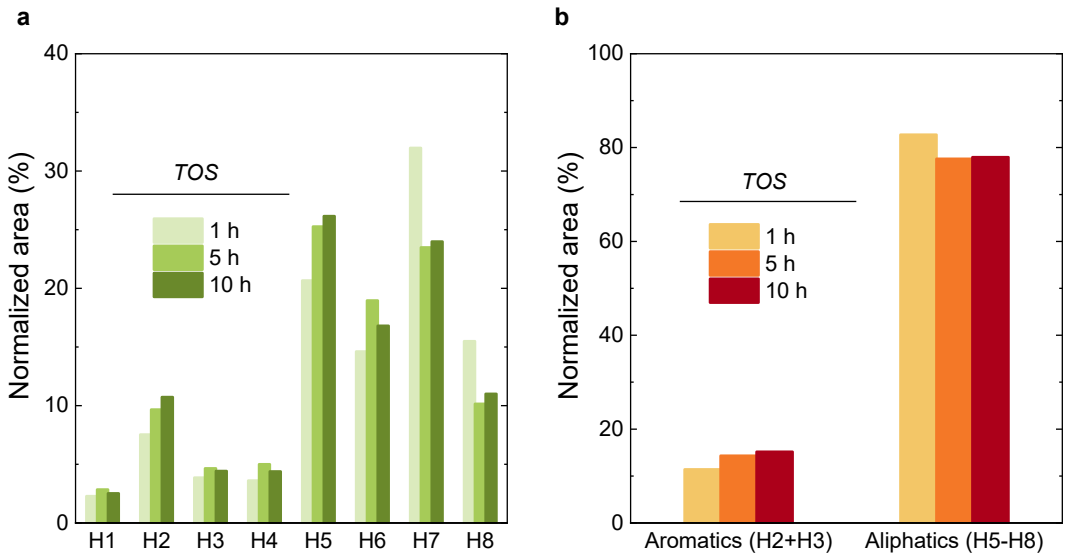

Figure S19 a) Specific type of protons by region and b) total aromatic and aliphatic hydrogens as calculated from integrating the ^{1}H NMR spectra (Figure S22) for the soluble cokes formed in the NiZ_{40} catalyst at different times on stream. The designations of the different types of protons are listed in Table S1.

Supplementary Tables

Table S1 Structural assignments for the integration of the soluble coke ^{1}H NMR spectra as reported by Poveda et al.[2]

Region (ppm)		**Structural assignment**
9.0-12.0	H_1	Aldehydic and carboxylic hydrogen
7.2-9.0	H_2	Aromatic hydrogen linked to aromatic carbons in di- or poly-aromatic rings
6.0-7.2	H_3	Aromatic hydrogen linked to mono-aromatic rings
4.5-6.0	H_4	Olefinic hydrogen
2.0-4.5	H_5	Paraffinic and naphthenic hydrogen (-CH, $-CH_2$, and $-CH_3$) linked to aromatic systems in α position
1.5-2.0	H_6	Naphthenic hydrogen ($-CH_2$), β to aromatic systems
1.0-1.5	H_7	Paraffinic hydrogen, β to aromatic systems, alkyl termination
0.1-1.0	H_8	Paraffinic hydrogen ($-CH_3$), γ and more to aromatic systems

Supplementary References

1 L. H. Ong, M. Dömök, R. Olindo, A. C. Van Veen and J. A. Lercher, *Microporous Mesoporous Mater.*, 2012, **164**, 9–20.

2 J. C. Poveda and D. R. Molina, *J. Pet. Sci. Eng.*, 2012, **84**–**85**, 1–7.